Phase transitions in the Hubbard model for the bismuth nickelate

Shoya Kojima, Joji Nasu, and Akihisa Koga
Department of Physics, Tokyo Institute of Technology, Meguro, Tokyo 152-8551, Japan
(Received 7 April 2016; revised manuscript received 14 June 2016; published 5 July 2016)

We study low temperature properties of the Hubbard model for the bismuth nickelate, where degenerate orbitals in the nickel ions and a single orbital in the bismuth ions are taken into account, combining dynamical mean-field theory with the continuous-time quantum Monte Carlo method. We discuss the effect of the attractive interactions to mimic the valence skipping phenomenon in the bismuth ions. We demonstrate how the charge and magnetically ordered states are stable against thermal fluctuations. It is furthermore clarified that the ferromagnetically ordered and orbital ordered states are stabilized due to the presence of the orbital degeneracy at low temperatures. The crossover between metallic and insulating states is also discussed.

DOI: 10.1103/PhysRevB.94.045103

I. INTRODUCTION

Transition-metal oxides provide the typical playground for strongly correlated electron systems. Interesting examples are the manganite $La_{1-x}Sr_xMnO_3$ [1] and the ruthenate Sr_2RuO_4 [2], where remarkable phenomena have been observed such as the colossal magnetoresistance and triplet superconductivity. These stimulate extensive theoretical and experimental investigations [3,4]. Common physics in the perovskite-type oxides is that the orbital degrees of freedom in the transition-metal ions (Mn, Ru) play a crucial role for realizing interesting low temperature properties. On the other hand, the lanthanum or strontium ions simply control electron number and play little role for interesting phenomena.

Recently, the bismuth nickelate $BiNiO_3$ has attracted current interest since the successful observation of the colossal negative thermal expansion [5]. In the compound, the phenomenon occurs together with the valence transition in the nickel and bismuth ions. In fact, it has been reported that, as increasing temperature and/or pressure, the electronic configuration $Bi^{3+}_{0.5}Bi^{5+}_{0.5}Ni^{2+}O^{2-}_3$ is suddenly changed to that $Bi^{3+}Ni^{3+}O^{2-}_3$. One of the important points in the compound is the orbital degeneracy in the nickel ions. This may induce interesting low temperature states such as the orbital ordered and ferromagnetically ordered states, which have not been observed up to now. Another is that the bismuth forms the compound with 3+ and 5+ valence states, so called, a "valence-skipping" ion. This behavior should be explained by considering fairly large attractive interactions between 6*s* electrons [6] although one naively expects that they are little correlated, comparing with 3*d* electrons in the nickel ions. Therefore, it is necessary to treat electron correlations in both ions correctly to understand low temperature properties in the compound.

Naka *et al.* have studied the single-band Hubbard model to discuss low temperature properties in the compound by means of the Hartree-Fock approximations [7]. The existence of the valence transition has been clarified, by considering the effective attractive interactions in the bismuth ions. However, the orbital degeneracy in the nickel ions has not been treated, and thereby low temperature properties in the compound still remain unclear. In particular, the orbital degrees of freedom and the Hund coupling should play a crucial role to understand the valence and magnetic transitions in the system. Therefore, it is necessary to treat the valence skipping in the bismuth ions as well as the orbital degeneracy in the nickel ions on equal footing.

To clarify the above issues, we study the Hubbard model composed of two distinct sites with degenerate orbitals for nickel ions and a single orbital for bismuth ions. Here, using dynamical mean-field theory [8–10], we discuss how local electron correlations in both ions affect low temperature properties. We then reveal the stability of the charge density wave (CDW) and antiferromagnetically (AFM) ordered states against thermal fluctuations. Furthermore, we find the ferromagnetically (FM) ordered state and the antiferroorbital (AFO) ordered state. Examining low energy properties in the density of states, we discuss the metal-insulator crossover in the system.

The paper is organized as follows. In Sec. II, we introduce the model for the compound $BiNiO_3$ and summarize our theoretical approach. In Sec. III, we discuss how the attractive interaction effectively realizes the valence skip in the bismuth ions. In Sec. IV, we obtain the phase diagrams to discuss the role of the degenerate orbitals at low temperatures. A summary is given in the last section.

II. MODEL AND METHOD

We study the effect of strong electron correlations in the compound $BiNiO_3$. The model should be described by the following Hubbard Hamiltonian,

$$H = H_{\rm Bi} + H_{\rm Ni} + H_{\rm Bi-Ni}, \tag{1}$$

$$H_{\rm Bi} = -t_{\rm Bi}\sum_{\langle ij\rangle\sigma}^{\rm Bi}(b^\dagger_{i\sigma}b_{j\sigma} + {\rm H.c.}) + U_{\rm Bi}\sum_i^{\rm Bi}\left(n^{\rm Bi}_{i\uparrow}-\frac{1}{2}\right)\left(n^{\rm Bi}_{i\downarrow}-\frac{1}{2}\right), \tag{2}$$

$$H_{\rm Ni} = -t_{\rm Ni}\sum_{\langle ij\rangle\alpha\sigma}^{\rm Ni}(a^\dagger_{i\alpha\sigma}a_{j\alpha\sigma} + {\rm H.c.}) + \Delta\sum_{i\alpha\sigma}^{\rm Ni} n^{\rm Ni}_{i\alpha\sigma} + U_{\rm Ni}\sum_{i\alpha}\left(n^{\rm Ni}_{i\alpha\uparrow}-\frac{1}{2}\right)\left(n^{\rm Ni}_{i\alpha\downarrow}-\frac{1}{2}\right)$$

$$+U'_{\rm Ni}\sum_{i\sigma}\left(n^{\rm Ni}_{i1\sigma}-\frac{1}{2}\right)\left(n^{\rm Ni}_{i2\bar{\sigma}}-\frac{1}{2}\right)$$

$$+(U'_{\rm Ni}-J)\sum_{i\sigma}\left(n^{\rm Ni}_{i1\sigma}-\frac{1}{2}\right)\left(n^{\rm Ni}_{i2\sigma}-\frac{1}{2}\right), \quad (3)$$

$$H_{\rm Bi-Ni}=-t'\sum_{\langle ij\rangle\alpha\sigma}(a^{\dagger}_{i\alpha\sigma}b_{j\sigma}+{\rm H.c.}), \quad (4)$$

where $b^{\dagger}_{i\sigma}$ ($b_{i\sigma}$) is a creation (annihilation) operator of an electron with spin σ at the Bi sites and $a^{\dagger}_{i\alpha\sigma}$ ($a_{i\alpha\sigma}$) is a creation (annihilation) operator of an electron with spin $\sigma(=\uparrow,\downarrow)$ and orbital index $\alpha(=1,2)$ at the Ni sites of the ith unit cell, $n^{\rm Bi}_{i\sigma}=b^{\dagger}_{i\sigma}b_{i\sigma}$, and $n^{\rm Ni}_{i\alpha\sigma}=a^{\dagger}_{i\alpha\sigma}a_{i\alpha\sigma}$. t_M is the hopping integral between $M(=$ Bi, Ni) ions and t' is between Ni and Bi ions (see Fig. 1). $U_{\rm Bi}(<0)$ is the onsite interaction in the Bi ions, and $U_{\rm Ni}$, $U'_{\rm Ni}$, and J are the intraorbital interaction, interorbital interaction, and Hund coupling in the Ni ions. In our paper, we neglect the spin flip and pair hopping terms, for simplicity. Δ is the energy difference between an e_g level in Ni ions and an s level in Bi ions, which should be tuned experimentally by the applied pressure. The effective model may be regarded to have the spatially alternating interactions [11] since electron correlations are taken into account in both nickel and bismuth ions.

The compound $BiNiO_3$ exhibits the CDW and AFM ordered states below the critical temperatures $T_c^{\rm CDW}$ and $T_c^{\rm AFM}$, where charges in Bi ions and spins in Ni ions are ordered, respectively [5]. Therefore, the lattices for Ni and Bi ions are assumed to be divided into two sublattices, which is schematically shown in Fig. 1. Each M ion in a sublattice A has nearest neighbor M ions in a sublattice B. On the other hand, each M ion is surrounded by $\bar{M}$ ions in both sublattices. Therefore, the hopping t' between different ions should yield a sort of frustration, which may suppress charge and magnetic fluctuations. The attractive onsite interaction in the Bi ions may induce an s-wave superconducting state. However, we do not assume this state in the present paper since it has not been observed in $BiNiO_3$ so far. This should be justified by the introduction of the intersite Coulomb repulsions [7].

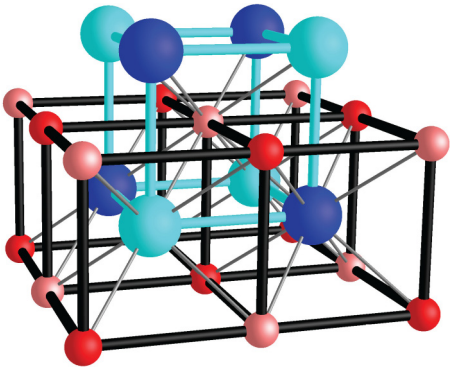

FIG. 1. Three dimensional lattice structure in the compound $BiNiO_3$. Grayscaled large (small) spheres represent the Bi (Ni) ions in the sublattice. The hopping integrals t_M (t') between the same (different) ions are expressed by the bold (thin) lines.

To discuss the stability of the ordered states, we make use of DMFT [8–10]. In DMFT, the original lattice model is mapped to an effective impurity model, where local electron correlations are accurately taken into account. The lattice Green's function is obtained via a self-consistency condition imposed on the impurity problem. This treatment is exact in infinite dimensions, and the DMFT method has successfully explained interesting physics such as Mott transitions [12–18] and magnetic transitions [19–22]. When the realistic condition is concerned, t_M is more dominant than t', which allows us to use the self-consistent equations for DMFT [19,20] as

$$(\mathcal{G}_{M\gamma})^{-1}=i\omega_n+\mu_M-\left(\frac{D_M}{2}\right)^2 G_{M\bar{\gamma}}$$

$$-\frac{1}{2}\left(\frac{D'}{2}\right)^2\sum_{\gamma'}G_{\bar{M}\gamma'}, \quad (5)$$

where $\omega_n=(2n+1)\pi T$ is the Matsubara frequency, T is the temperature, $\mu_{\rm Ni}=\mu-\Delta$, $\mu_{\rm Bi}=\mu$, and μ is the chemical potential. $\mathcal{G}_{M\gamma}$ ($G_{M\gamma}$) is the noninteracting (full) Green's function for the M ion in the $\gamma(=A,B)$th sublattice. For convenience, we neglect spin and orbital indexes in Eq. (5), and consider the Bethe lattice with coordination $z\to\infty$ as a lattice structure, where the hoppings are rescaled as $D_M=2\sqrt{z}t_M$ and $D'=2\sqrt{z}t'$. In the framework of DMFT, we solve effective impurity models for Bi and Ni sites. To discuss finite temperature properties in the system, we employ the strong-coupling version of the continuous-time quantum Monte Carlo method [23,24], which is efficient to study the Hubbard model in both weak and strong coupling regimes.

There are some possible ordered states at low temperatures. In the bismuth sites, the attractive interaction $U_{\rm Bi}(<0)$ should induce the CDW state. As for the nickel sites, the repulsive interactions $(U_{\rm Ni},U'_{\rm Ni},J)$ should stabilize the ferromagnetically (FM) or AFM ordered state. Furthermore, the ferroorbital (FO) or antiferroorbital (AFO) ordered state is also realizable, depending on the local electron fillings. To characterize the above states, we here define the order parameters as

$$m^{\rm Bi}_{\rm CDW}=\tfrac{1}{2}\langle n^{\rm Bi}_A-n^{\rm Bi}_B\rangle, \quad (6)$$

$$m^{\rm Ni}_{\rm FM(AFM)}=\tfrac{1}{4}\langle S^z_A\pm S^z_B\rangle, \quad (7)$$

$$m^{\rm Ni}_{\rm FO(AFO)}=\tfrac{1}{2}\langle T^z_A\pm T^z_B\rangle, \quad (8)$$

where $n^{\rm Bi}_{\gamma}=\sum n^{\rm Bi}_{\gamma\sigma}/2$ is a local filling at the Bi sites, $S^z_{\gamma}=\sum_{\alpha}(n^{\rm Ni}_{\alpha\uparrow\gamma}-n^{\rm Ni}_{\alpha\downarrow\gamma})/2$, and $T^z_{\gamma}=\sum_{\sigma}(n^{\rm Ni}_{1\sigma\gamma}-n^{\rm Ni}_{2\sigma\gamma})/2$ are the z component of the spin and pseudospin at Ni sites in the γth sublattice. Here, we focus on the above diagonal orders to discuss their stabilities. We also calculate the following quantity:

$$\tilde{A}_M=-\frac{1}{\pi T}G_M\left(\frac{1}{2T}\right). \quad (9)$$

This quantity is reduced to the density of states for M ions at the Fermi level in the limit $T\to 0$ [25], which should allow us to discuss how the metallic state ($\tilde{A}\neq 0$) competes with the

insulating state ($\tilde{A} = 0$) at finite temperatures. In the paper, we use the hopping $D(=D_{\rm Ni} = D_{\rm Bi})$ as the unit of energy and fix the parameters as $U_{\rm Ni} = U'_{\rm Ni} + 2J$, $U_{\rm Ni}/J = 0.1$, and $D'/D = 0.28$, which are based on Refs. [3,7,26,27]. The total electron density is fixed as $\sum_\sigma (n^{\rm Bi}_{\sigma\gamma} + \sum_\alpha n^{\rm Ni}_{\alpha\sigma\gamma}) = 2$ for each sublattice γ. The model Hamiltonian Eq. (1) is equivalent under the particle-hole transformations except for the sign of the parameter Δ. Therefore, our discussions are restricted to the case with $\Delta \geqslant 0$ without loss of generality.

III. EFFECT OF ATTRACTIVE INTERACTIONS

We discuss the effect of the attractive interaction $U_{\rm Bi}$. In the previous paper [7], the interaction $U_{\rm Bi}$ has been taken into account within the Hartree-Fock approximation. In this approximation, the valence skipping nature appears only in the charge-density-wave (CDW) phase, and the interaction has no effects in the paramagnetic state. On the other hand, the valence skip in the bismuth ions always appears in the real material [5]. To discuss how such a condition is realized by the attractive interaction, we examine empty, singly, and doubly occupied states in the Bi site at certain parameters. Figure 2(a) shows their probabilities as a function of the attractive interaction $U_{\rm Bi}$. In the parameter set used in Fig. 2, the local band filling for Bi sites are always half filled (not shown). When $U_{\rm Bi} = 0$, all possible states are equally realized with $e = s_\sigma = d = 1/4$. The introduction of the attractive interaction favors empty and doubly occupied states, while decreasing the probability for singly occupied states. It is found that the singly occupied state is little realized ($s_\sigma < 0.04$) when $U_{\rm Bi}/D < -2.5$. We show the temperature dependence in the system with $U_{\rm Bi}/D = -3$ in the inset of Fig. 2(a). At high temperatures ($T > |U_{\rm Bi}|$), the local band filling is away from half filling and the single occupied states are realized with $s_\sigma \sim 0.2$. Therefore, we cannot discuss the valence skipping phenomenon in the case. On the other hand, when $T/D < 0.1(\ll |U_{\rm Bi}/D|)$, the single occupancy is negligible and little depends on the temperature. Furthermore, the single occupancy little depends on the energy difference Δ although the local band filling for the Bi sites and the probabilities for the empty and doubly occupied states are gradually changed, as shown in Fig. 2(b). Therefore, the Bi site can be regarded as the valence skipping one when we fix the attractive interaction as $U_{\rm Bi}/D = -3$ and focus on low temperature properties ($T/D < 0.1$). In the following, we fix the attractive interaction $U_{\rm Bi}/D = -3$. To proceed our discussions under the realistic conditions for critical temperatures ($T_c^{\rm AFM} < T_c^{\rm CDW}$), we consider two choices of the onsite Coulomb interaction as $U_{\rm Ni}/D = 1$ and $U_{\rm Ni}/D = 10$ in the following.

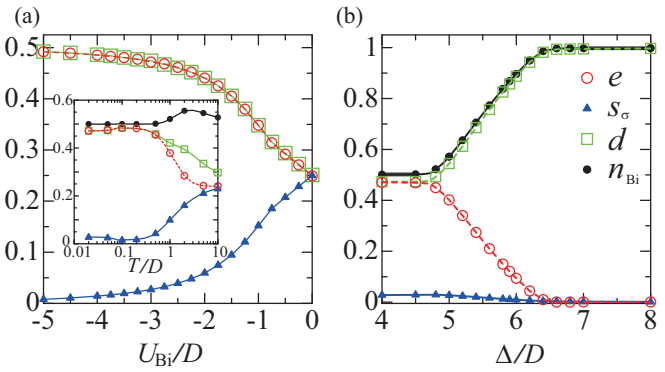

FIG. 2. (a) The probabilities for empty, singly, and doubly occupied states in the Bi states in the system with $U_{\rm Ni}/D = 10$ and $\Delta/D = 2$ when $T/D = 0.04$ (main panel) and $U_{\rm Bi}/D = -3$ (inset). (b) The probabilities as a function of Δ when $U_{\rm Ni}/D = 10$, $U_{\rm Bi}/D = -3$, and $T/D = 0.04$.

IV. LOW TEMPERATURE PROPERTIES

First, we would like to discuss low temperature properties in the weak coupling case with $U_{\rm Ni}/D = 1$. By performing DMFT calculations at a temperature $T/D = 0.02$, we obtain the results, as shown in Fig. 3. When $\Delta = 0$, both Ni and Bi ions are half filled ($n_{\rm Bi} = n_{\rm Ni} = 0.5$). We find that the CDW and AFM ordered states appear with large order parameters $m^{\rm Bi}_{\rm CDW} = 0.46$ and $m^{\rm Ni}_{\rm AFM} = 0.45$. Figures 3(b) and 3(c) show the square of the order parameters, for discussions of the critical phenomena. The magnetic moments in two orbitals of the Ni sites are parallel due to the existence of the

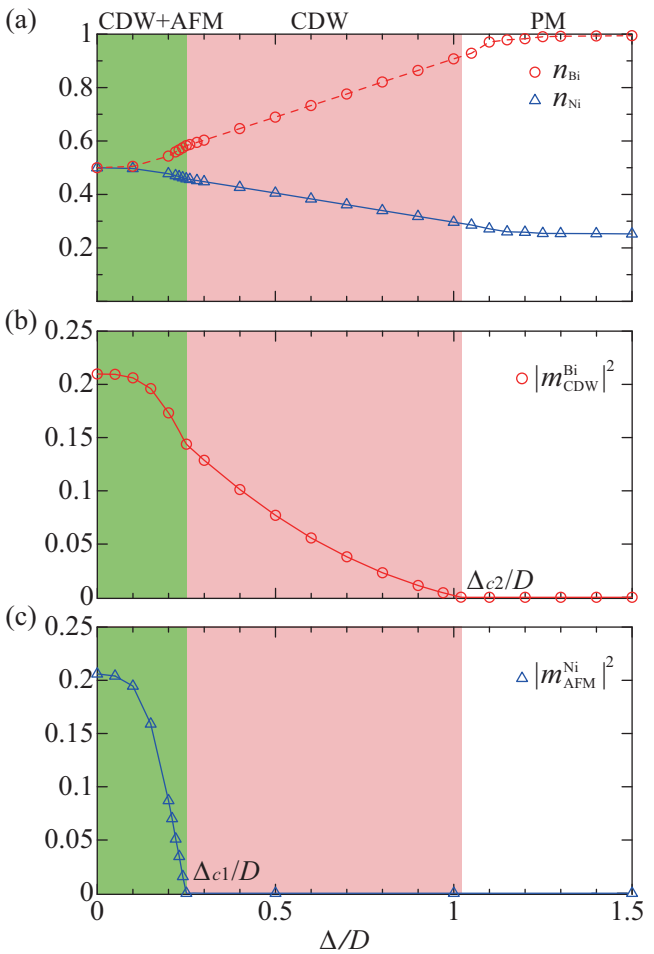

FIG. 3. Δ dependences of (a) the local filling and the square of the order parameters in (b) the Bi and (c) Ni sites as in the system with $U_{\rm Ni}/D = 10$ when $T/D = 0.02$.

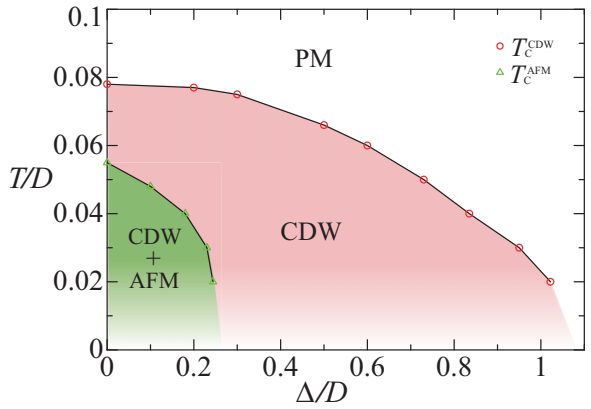

FIG. 4. Phase diagram in the weak coupling case with $U_{Ni}/D = 1$. Circles (triangles) represent the second-order phase transition points, where the CDW (AFM) order parameter vanishes.

Hund coupling. Introducing Δ, the number of electrons in Ni (Bi) sites gradually decreases (increases), and both order parameters decrease. At $\Delta = \Delta_{c1}$, the AFM order parameter vanishes and the second-order phase transition occurs to a genuine CDW state. We note that the hopping t' simply suppresses magnetic and charge fluctuations and does not induce the cooperating phenomena between the Ni and Bi ions. Therefore, the AFM and CDW states independently appear in the model although a singularity appears in some curves of physical quantities. Further increase in Δ decreases the CDW order parameter, and finally m^{Bi}_{CDW} vanishes at $\Delta = \Delta_{c2}$. By examining critical behavior of the order parameters, $m \sim |\Delta - \Delta_c|^\beta$ with the exponent $\beta = 1/2$, we obtain the critical values as $\Delta_{c1}/D \sim 0.25$ and $\Delta_{c2}/D \sim 1.0$, as shown in Figs. 3(b) and 3(c). In the large Δ region, the paramagnetic (PM) state is realized, where the Bi sites are almost fully occupied and the Ni sites are quarter filled, as shown in Fig. 3(a).

By performing similar calculations, we obtain the phase diagram as shown in Fig. 4. We find that the CDW state is widely stabilized in the phase diagram, where the empty and doubly occupied states are alternately realized in the Bi sites. On the other hand, the AFM ordered state is realized in the Ni ions at lower T and the smaller Δ region, as shown in Fig. 4. In the weak coupling case, the phase diagram is essentially the same as that obtained in the previous paper [7].

Let us move to the strong coupling case with $U_{Ni}/D = 10$. It is known that most nickelates show insulating behavior with magnetism at low temperatures, where charge degrees of freedom are frozen due to strong electron correlations. Therefore, the strong coupling case should be also analyzed to discuss the relevance to the compound $BiNiO_3$. Figure 5 shows the filling and order parameters at the low temperature $T/D = 0.02$. When $\Delta/D \lesssim 5$, both Bi and Ni sites are half filled, and the CDW and AFM states are stabilized, as discussed above. Around $\Delta/D \sim 5$, the local electron number is changed and the staggered spin moment decreases rapidly. This makes the AFM state unstable and the phase transition occurs in the Ni sites although the CDW state remains in the Bi sites. At $T/D = 0.02$, this nonmagnetic state is realized in a tiny region, which may be invisible in Fig. 5. Further increase in Δ induces

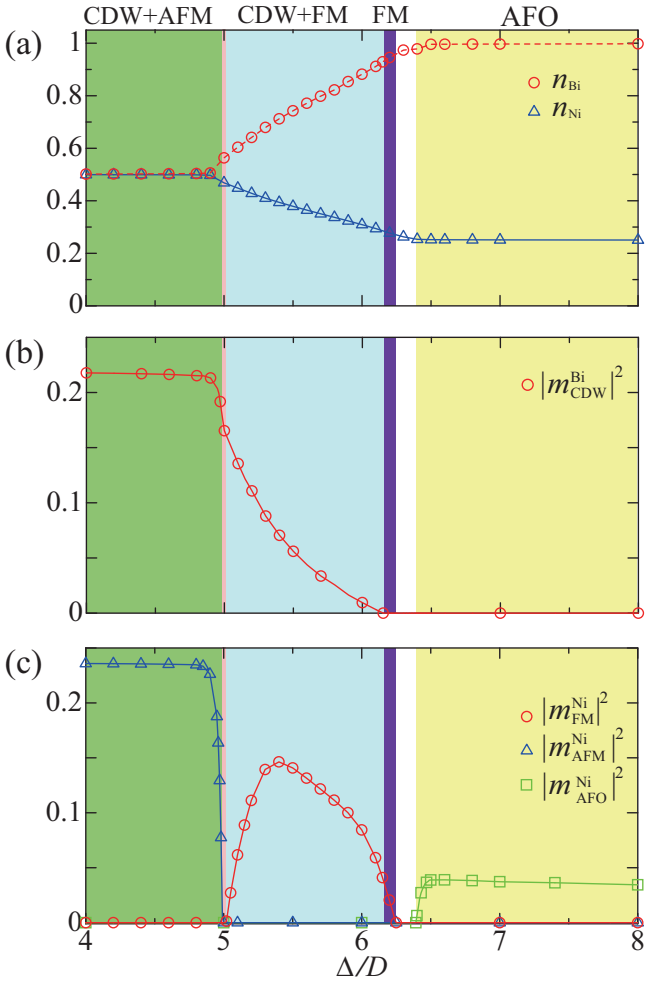

FIG. 5. Δ dependences of (a) the local filling and the square of the order parameters in (b) the Bi and (c) Ni sites in the system with $U_{Ni}/D = 10$ when $T/D = 0.02$.

the uniform spin moment in the Ni sites m^{Ni}_{FM}, and the FM state is instead realized. In the state, the number of electrons in the Ni site is intermediate and no orbital moment appears. This is consistent with the fact that the ferromagnetic metallic ground state is stabilized between quarter and half fillings in the degenerate Hubbard model [21]. When $n_{Bi} \to 1$ and $n_{Ni} \to 1/4$, we find that the CDW and FM order parameters vanish at $\Delta/D = 6.2$ and $\Delta/D = 6.3$, respectively. When $\Delta/D \sim 6.4$, the staggered orbital moment is induced rapidly and the AFO state is realized. As the AFO state does not appear in the weak coupling case, we conclude that the state is stabilized due to the strong Coulomb interaction in the model with degenerate orbitals. The larger value of Δ tends to fix the electron number as $n_{Bi} = 1$ and $n_{Ni} = 1/4$, and hence the order parameter becomes constant.

The phase diagram is shown in Fig. 6. In the small Δ region, there appear the CDW and AFM states. In the case with $U_{Ni}/D = 10$, the critical temperatures are little changed since the local band filling in each ion is fixed to be commensurate due to strong electron correlations in Ni ions. When $\Delta \sim 5.5 (\Delta > 6.5)$, the FM (AFO) ordered state

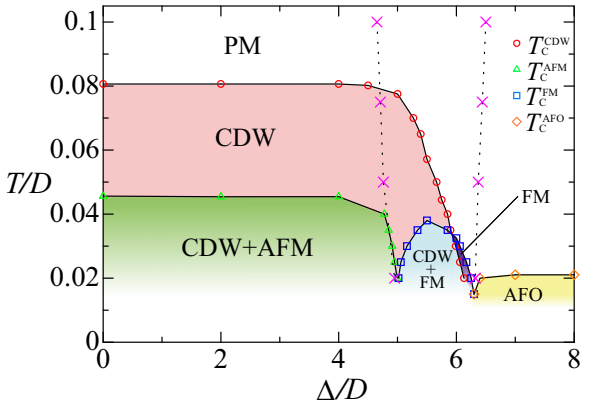

FIG. 6. Phase diagram in the strong coupling case with $U_{\rm Ni}/D = 10$. Circles, triangles, squares, and diamonds represent the phase transition points, where the CDW, AFM, FM, and AFO order parameter vanishes, respectively. Crosses represent the metal-insulator crossover points (see text).

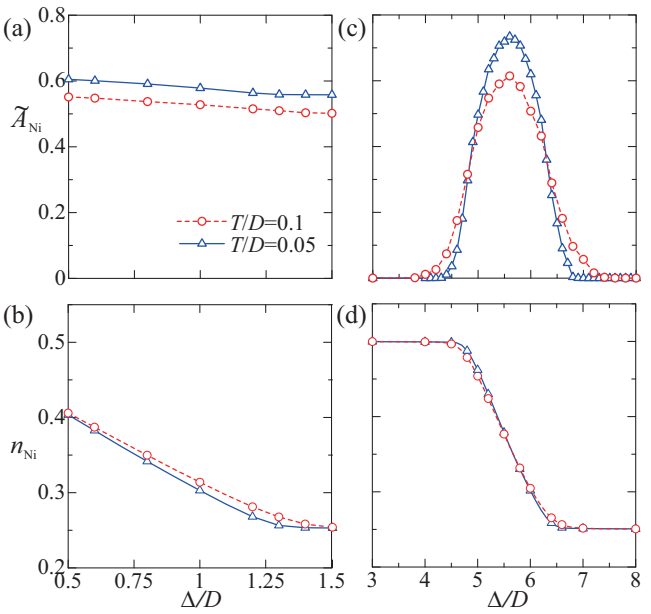

FIG. 7. Δ dependences of (a) the density of states at the Fermi level $\tilde{A}_{\rm Ni}$ and (b) the local filling $n_{\rm Ni}$ at Ni sites in the weak coupling case with $U_{\rm Ni}/D = 1$. (c), (d) Corresponding data for the strong coupling case with $U_{\rm Ni}/D = 10$.

appears at low temperatures. It is expected that in the large Δ case, the decrease of the temperature enhances ferromagnetic correlations, which induces the FM-AFO state with $m^{\rm Ni}_{\rm FM} \neq 0$ and $m^{\rm Ni}_{\rm AFO} \neq 0$ [21]. In the present study, we examine the Hubbard model with single-orbital sites and degenerate-orbital sites, taking into account the valence skipping nature and strong electron correlations. The obtained phase diagram is consistent with the experiments [5], although the FM and AFO ordered states have not been observed. We could not obtain the converged solutions within our numerical accuracy at very low temperatures $T/D \lesssim 0.01$. It is an intriguing problem to clarify ground state properties in the strong coupling case, which is left for future work.

Finally, we discuss metallic state properties in the system. When $T/D = 0.05$, the second-order phase transition occurs between the CDW and PM states at $\Delta/D = 0.73$ (5.7) in the weak (strong) coupling case. In our calculations, the attractive interaction $U_{\rm Bi}$ is fixed to realize the valence skip phenomenon in the bismuth ions, and the excitation gap in the one particle spectrum always opens in the bismuth sites. Here, we focus on metallic properties at the Ni sites in the system close to the phase boundary for the CDW state. The density of states at the Fermi level $\tilde{A}_{\rm Ni}$ and the local band filling $n_{\rm Ni}$ are shown in Fig. 7. In the weak coupling case, $\tilde{A}_{\rm Ni}$ is almost constant although the local band filling $n_{\rm Ni}$ is gradually changed. Therefore, the metallic state is always stable in the case. On the other hand, in the strong coupling case, different behavior appears. When $\Delta/D \lesssim 4$, the local electron number at the Ni sites is fixed as half filling. As the Coulomb interaction at the nickel sites is fairly large, we can say that the Mott insulator is realized with $\tilde{A}_{\rm Ni} \sim 0$. When $4.5 \lesssim \Delta/D \lesssim 6.5$, the intermediate filling is realized and metallic behavior appears with finite $\tilde{A}_{\rm Ni}$. Increasing Δ, the local band filling approaches quarter in the nickel sites. Then, Mott insulating behavior appears again with $\tilde{A}_{\rm Ni} \sim 0$, as shown in Fig. 7(c). Since we could not find any singularities in the curves, the crossover occurs between the metallic state and two Mott insulating states. The latter states are stabilized at local commensurate fillings, in contrast to the weak coupling case. This crossover is not directly related to the phase transition in the Bi sites. In fact, at higher temperatures ($T/D = 0.1$), the CDW state is not realized, but crossover behavior still remains, as shown in Fig. 7. The crossover points, which may be deduced roughly under the conditions $n_{\rm Ni} = 0.26$ and 0.49, are shown as the crosses in Fig. 6. We find that the metal-insulator crossover little depends on the temperature, in contrast to the phase boundary for the CDW state. As temperatures decrease, the crossover approaches the phase boundary for the FM state since the AFM and AFO states are realized only at the commensurate fillings and the FM state is realized in between, as discussed above. Unfortunately, the valence transition in the compound $BiNiO_3$ between the electronic configurations $Bi^{3+}_{0.5}Bi^{5+}_{0.5}Ni^{2+}O^{2-}_3$ and $Bi^{3+}Ni^{3+}O^{2-}_3$ is of first order and the metal-insulator transition simultaneously occurs [5,28]. This discrepancy may originate from the fact that the valence transition in the compound is accompanied by the structure phase transition associated with a volume shrinkage or a strong mixing between the Ni $3d$ and ligand orbitals, which is often expected for perovskite nickelates [29]. Therefore, the first-order phase transitions must be explained when one considers the valence dependent hopping integrals, ligand orbitals, electron-phonon coupling, etc, which is now under consideration.

V. SUMMARY

We have studied the Hubbard model for the compound $BiNiO_3$, where single (degenerate) orbital in the Bi (Ni) ions is taken into account. Combining dynamical mean-field theory with the continuous-time quantum Monte Carlo method, we

have discussed the finite temperature properties in the system. It has been clarified how the valence skip phenomenon in the bismuth sites is described by the attractive interactions. By performing the DMFT calculations systematically, we have obtained the phase diagrams, where the ferromagnetically ordered and orbital ordered states appear in addition to the charge density wave and antiferromagnetically ordered states observed experimentally. We have also discussed the crossover between metallic and insulating states.

ACKNOWLEDGMENTS

We would like to thank M. Naka for valuable discussions. Parts of the numerical calculations are performed in the supercomputing systems in ISSP, the University of Tokyo. This work was partly supported by the Grant-in-Aid for Scientific Research from JSPS, KAKENHI Grant No. 25800193, No. 16H01066 (A.K.), and No. 16K17747 (J.N.). The simulations have been performed using some of the ALPS libraries [30].

[1] Y. Tokura, A. Urushibara, Y. Moritomo, T. Arima, A. Asamitsu, G. Kido, and N. Furukawa, J. Phys. Soc. Jpn. **63**, 3931 (1994).
[2] Y. Maeno, H. Hashimoto, K. Toshida, S. Nishizaki, T. Fujita, J. G. Bednorz, and F. Lichtenberg, Nature (London) **372**, 532 (1994).
[3] M. Imada, A. Fujimori, and Y. Tokura, Rev. Mod. Phys. **70**, 1039 (1998); Y. Tokura and N. Nagaosa, Science **288**, 462 (2000).
[4] T. M. Rice and M. Sigrist, J. Phys. Condens. Matter **7**, L643 (1995).
[5] M. Azuma, W. Chen, H. Seki, M. Czapski, S. Olga, K. Oka, M. Mizumaki, T. Watanuki, N. Ishimatsu, N. Kawamura, S. Ishiwata, M. G. Tucker, Y. Shimakawa, and J. P. Attfield, Nat. Commun. **2**, 347 (2011).
[6] C. M. Varma, Phys. Rev. Lett. **61**, 2713 (1988).
[7] M. Naka, H. Seo, and Y. Motome, Phys. Rev. Lett. **116**, 056402 (2016).
[8] W. Metzner and D. Vollhardt, Phys. Rev. Lett. **62**, 324 (1989).
[9] A. Georges, G. Kotliar, W. Krauth, and M. J. Rozenberg, Rev. Mod. Phys. **68**, 13 (1996).
[10] T. Pruschke, M. Jarrell, and J. K. Freericks, Adv. Phys. **44**, 187 (1995).
[11] T. Saitou, A. Koga, and A. Yamamoto, J. Supercond Nov Magn **26**, 1771 (2013); A. Koga, T. Saitou, and A. Yamamoto, J. Phys. Soc. Jpn. **82**, 024401 (2013).
[12] M. Caffarel and W. Krauth, Phys. Rev. Lett. **72**, 1545 (1994).
[13] Th. Pruschke, D. L. Cox, and M. Jarrell, Phys. Rev. B **47**, 3553 (1993).
[14] O. Sakai and Y. Kuramoto, Solid State Commun. **89**, 307 (1994).
[15] R. Bulla, Phys. Rev. Lett. **83**, 136 (1999).
[16] A. Georges, G. Kotliar, and W. Krauth, Z. Phys. B **92**, 313 (1993).
[17] Y. Ono, R. Bulla, and A. C. Hewson, Eur. Phys. J. B **19**, 375 (2001); Y. Ohashi and Y. Ono, J. Phys. Soc. Jpn. **70**, 2989 (2001).
[18] A. Koga, Y. Imai, and N. Kawakami, Phys. Rev. B **66**, 165107 (2002); A. Koga, N. Kawakami, T. M. Rice, and M. Sigrist, Phys. Rev. Lett. **92**, 216402 (2004).
[19] R. Chitra and G. Kotliar, Phys. Rev. Lett. **83**, 2386 (1999).
[20] R. Zitzler, N.-H. Tong, T. Pruschke, and R. Bulla, Phys. Rev. Lett. **93**, 016406 (2004).
[21] T. Momoi and K. Kubo, Phys. Rev. B **58**, R567 (1998).
[22] H. Yanatori and A. Koga, J. Phys. Soc. Jpn. **85**, 014002 (2015).
[23] P. Werner, A. Comanac, L. déMedici, M. Troyer, and A. J. Millis, Phys. Rev. Lett. **97**, 076405 (2006).
[24] E. Gull, A. J. Millis, A. N. Rubtsov, A. I. Lichtenstein, M. Troyer, and P. Werner, Rev. Mod. Phys. **83**, 349 (2011).
[25] E. G. C. P. van Loon, A. I. Lichtenstein, M. I. Katsnelson, O. Parcollet, and H. Hafermann, Phys. Rev. B **90**, 235135 (2014).
[26] M. Azuma, S. Carlsson, J. Rodgers, M. G. Tucker, M. Tsujimoto, S. Ishiwata, S. Isoda, Y. Shimakawa, M. Takano, and J. P. Attfield, J. Am. Chem. Soc. **129**, 14433 (2007).
[27] T. Mizokawa and A. Fujimori, Phys. Rev. B **54**, 5368 (1996).
[28] S. Ishiwata, M. Azuma, and M. Takano, Solid State Ionics **172**, 569 (2004).
[29] S. Ishiwata, M. Azuma, M. Hanawa, Y. Moritomo, Y. Ohishi, K. Kato, M. Takata, E. Nishibori, M. Sakata, I. Terasaki, and M. Takano, Phys. Rev. B **72**, 045104 (2005).
[30] B. Bauer, L. D. Carr, H. G. Evertz, A. Feiguin, J. Freire, S. Fuchs, L. Gamper, J. Gukelberger, E. Gull, S. Guertler, A. Hehn, R. Igarashi, S. V. Isakov, D. Koop, P. N. Ma, P. Mates, H. Matsuo, O. Parcollet, G. Pawłowski, J. D. Picon, L. Pollet, E. Santos, V. W. Scarola, U. Schollwöck, C. Silva, B. Surer, S. Todo, S. Trebst, M. Troyer, M. L. Wall, P. Werner, and S. Wessel, J. Stat. Mech. (2011) P05001.